

SUPPORTING INFORMATION

This appendix formulates the mathematical model described in the main text. The initial conditions of the model, which include the effects of the blast, thermal and prompt radiation as well as the spatial population distribution, are described in §1. The radiation fallout model is provided in §2. The self-evacuation model and the delayed evacuation model are constructed in §3-§4. The figures contain results that are cited in the main text.

1 Initial Conditions

In this section, we quantify the initial spatial effects of the detonation, which is a 10-kt blast (with 5 kg of highly enriched uranium) at ground level with a fission fraction of 1.0 [1]. This event occurs on a weekday at 10 am on the Mall in Washington, D.C., where the wind is blowing from the west-southwest at 10 mph [1]. Throughout, we let t denote time (in hours), where the blast occurs at $t = 0$, and let (x, y) denote the spatial location relative to the location $(0,0)$ of the blast. We also let $r = \sqrt{x^2 + y^2}$ be the distance from the blast.

The ultimate goal of this section is to determine the fraction of people at a distance r from the blast who die ($P_f(r)$) and who are seriously injured ($P_i(r)$) due to the initial blast, thermal and prompt radiation effects (all three of these effects occur in a spatially symmetric manner). Because people can die or be injured from any subset of these effects, we determine the probability of dying or being injured from each of the three effects in isolation in §1.1-§1.3, and then we combine them probabilistically to determine the total death and injury probabilities in §1.4. Finally, we describe the spatial population density in §1.5, which allows us to compute the number of dead or injured people in each location. Note that subsequent deaths and injuries due to radiation fallout are not included in the calculations in this section.

1.1 Blast Effects

The blast wave is 50% of the total energy from the detonation. The goal of this subsection is to compute $P_f(\text{blast}|r)$ and $P_i(\text{blast}|r)$, which are the probabilities of dying or being seriously injured from the blast effects when at a distance r from the detonation. The natural way to compute these quantities is to first specify the peak overpressure (measured in pounds per square inch, abbreviated by psi) at a distance r from the blast (e.g., using data from Figs. 3.73a,b,c in [2] or pages 1-15 and 1-16 of [1]), and then determine the effects from the overpressure. However, as explained below, data in [1] allow us to directly compute the effects as a function of r .

The probability of death or injury from the blast depends upon whether a person is inside or outside at the time of the blast, the type of building they are in, and the severity of the damage to the building. As in [1], we assume that 85% of people are inside and 15% are outside at $t = 0$.

We begin with people who are inside, and use the lower left plot and lower right plot in Fig. 1-2 of [1], which for five types of buildings gives the probability of severe damage and the probability of either moderate or severe damage, respectively, as a function of r . We crudely estimate that 70% of the people inside are in concrete buildings and 30% are in a S1-type building from Fig. 1-2 of [1] (multi-story, wall-bearing building; brick apartment; 1-3 stories), based on a 1965 reference that has a 50-50 split between these building types for a large city ([3], Table 47). In §1.4, we find that $P_f(r)$ and $P_i(r)$ are extremely insensitive to the mix of buildings that we assume, because the blast effects are largely overshadowed by the burn effects and (to a lesser extent) the prompt radiation effects.

We model the probability of damage as a function of r as a complementary lognormal cumulative distribution function, which is flexible enough to capture the sigmoid behavior of most dose-response curves. We have four curves to fit, depending upon whether the damage

is severe or at least moderate, and whether the building is of type S1 or concrete. We begin with the probability of severe damage to a S1-type building, which is

$$P(\text{severe damage}|r, \text{S1}) = \frac{1}{2} - \frac{1}{2}\text{erf}\left(\frac{\ln(r) - \alpha_{s,\text{S1}}}{\sqrt{2}\beta_{s,\text{S1}}}\right), \quad (1)$$

where $\text{erf}(x)$ is the error function, and where $\alpha_{s,\text{S1}}$ and $\beta_{s,\text{S1}}$ can be expressed in terms of the distances that lead to 50% and 90% chance of severe damage ($D_{50}^{s,\text{S1}}$ and $D_{90}^{s,\text{S1}}$, respectively - these can be estimated directly from Fig. 1-2 in [1]) via

$$\alpha_{s,\text{S1}} = \ln(D_{50}^{s,\text{S1}}), \quad (2)$$

$$\beta_{s,\text{S1}} = \frac{\ln(D_{90}^{s,\text{S1}}) - \alpha_{s,\text{S1}}}{\sqrt{2}\text{erf}^{-1}(-0.8)}. \quad (3)$$

As explained in [4], the quantities in Fig. 1-2 of [1], which are based on [5], underestimate the D_{50} and D_{90} distances by $\approx 30\%$ because they are based on Cold War assumptions of assured target defeat rather than the vulnerability of buildings subject to an attack. Therefore, after estimating $D_{50}^{s,\text{S1}}$ and $D_{90}^{s,\text{S1}}$ from the lower left plot of figure 1-2, we inflate them by 30% to get $D_{50}^{s,\text{S1}} = 1.25$ km and $D_{90}^{s,\text{S1}} = 1.07$ km.

Similarly, using the lower right plot of Fig. 1-2 of [1] (and changing notation from s to m , we find that the probability of severe or moderate damage of a S1-type building is $\frac{1}{2} - \frac{1}{2}\text{erf}\left(\frac{\ln(r) - \alpha_{m,\text{S1}}}{\sqrt{2}\beta_{m,\text{S1}}}\right)$, where $D_{50}^{m,\text{S1}} = 1.30$ km and $D_{90}^{m,\text{S1}} = 1.08$ km. Hence, the probability of moderate damage to a S1-type building is

$$P(\text{moderate damage}|r, \text{S1}) = \frac{1}{2}\text{erf}\left(\frac{\ln(r) - \alpha_{s,\text{S1}}}{\sqrt{2}\beta_{s,\text{S1}}}\right) - \frac{1}{2}\text{erf}\left(\frac{\ln(r) - \alpha_{m,\text{S1}}}{\sqrt{2}\beta_{m,\text{S1}}}\right). \quad (4)$$

We now apply the same method for concrete buildings. Table 3.2-2 in the 2003 version of [2] has D_{50} distances for structural damage for 8 building types (page 131 describes how these buildings compare to those in the U.S.), showing that concrete buildings are $\approx 30\%$ stronger than buildings of type S4 in Fig. 1-2 of [1]. Because the 30% deflation of these distances for type S4 would exactly offset the 30% inflation of these distances required by

the comments in [4], we simply use the D_{50} and D_{90} values for S4-type buildings in Fig. 1-2 of [1] to estimate the damage function to concrete buildings. The analogs to equations (1) and (4) for concrete buildings are

$$P(\text{severe damage}|r, \text{concrete}) = \frac{1}{2} - \frac{1}{2} \operatorname{erf} \left(\frac{\ln(r) - \alpha_{s,\text{concrete}}}{\sqrt{2}\beta_{s,\text{concrete}}} \right), \quad (5)$$

$$P(\text{moderate damage}|r, \text{concrete}) = \frac{1}{2} \operatorname{erf} \left(\frac{\ln(r) - \alpha_{s,\text{concrete}}}{\sqrt{2}\beta_{s,\text{concrete}}} \right) - \frac{1}{2} \operatorname{erf} \left(\frac{\ln(r) - \alpha_{m,\text{concrete}}}{\sqrt{2}\beta_{m,\text{concrete}}} \right), \quad (6)$$

where $D_{50}^{s,\text{concrete}} = 0.44$ km, $D_{90}^{s,\text{concrete}} = 0.35$ km, $D_{50}^{m,\text{concrete}} = 0.54$ km, and $D_{90}^{m,\text{concrete}} = 0.45$ km.

The final step to computing the indoor casualty probabilities is to determine the probability of death or injury due to blast inside a concrete or S1-type building. According to paragraph 12.22 in [2], the casualty numbers inside (moderately and severely damaged) concrete buildings given in the “Killed Outright” and “Serious Injury (hospitalization)” columns in Table 12.21 of [2] are overall casualty numbers from Japan, and approximately half of those casualties were early and hence can be attributed to direct and indirect blast injuries (the remaining casualties were delayed and due to thermal effects or prompt radiation). Because 88% were killed in severely-damaged buildings and 14% were killed in moderately-damaged buildings (Table 12.21 in [2]), we set the blast fatality probabilities to $P_f(\text{blast} | \text{severe damage, concrete}) = 0.44$ and $P_f(\text{blast} | \text{moderate damage, concrete}) = 0.07$. Table 12.21 of [2] also states that 11% of people in severely-damaged buildings were seriously injured and 18% in moderately-damaged buildings were seriously injured. Assuming that the likelihood of blast injury is independent of whether or not someone died from thermal effects or prompt radiation, and that half of these injuries were due to blast effects (paragraph 12.22 in [2]), we have that $P_i(\text{blast} | \text{severe damage, concrete}) = \frac{0.11/2}{1-0.88}(1 - 0.44) = 0.26$, and $P_i(\text{blast} | \text{moderate damage, concrete}) = \frac{0.18/2}{1-0.14}(1 - 0.07) = 0.10$.

To estimate these probabilities for S1-type buildings, we use Table 10-1 in [5] (based on high-explosives data for brick houses in England) and obtain $P_f(\text{blast} \mid \text{severe damage, S1}) = 0.25$, $P_f(\text{blast} \mid \text{moderate damage, S1}) = 0.05$, $P_i(\text{blast} \mid \text{severe damage, S1}) = 0.2$, and $P_i(\text{blast} \mid \text{moderate damage, S1}) = 0.1$.

Finally, we compute the casualty probabilities for people who are outside at the time of the blast. We assume all people who are outside are near a building, and fit a complementary lognormal cdf function to the two ‘‘Translation Near Structures’’ curves (one for 50% casualties and one for 1% casualties) in Fig. 12.49 of [2], using the scaling law on page 558 of [2]. Assuming all of these casualties are fatalities, we obtain

$$P_i(\text{blast}|r, \text{outside}) = 0, \quad (7)$$

$$P_f(\text{blast}|r, \text{outside}) = \frac{1}{2} - \frac{1}{2} \operatorname{erf} \left(\frac{\ln(r) - \alpha_{\text{outside}}}{\sqrt{2}\beta_{\text{outside}}} \right), \quad (8)$$

where

$$\alpha_{\text{outside}} = \ln(D_{50}^{\text{outside}}) \quad (9)$$

$$\beta_{\text{outside}} = \frac{\ln(D_1^{\text{outside}}) - \alpha_{\text{outside}}}{\sqrt{2}\operatorname{erf}^{-1}(0.98)} \quad (10)$$

and $D_{50}^{\text{outside}} = 690 \times 10^{0.4}\text{ft} = 0.53 \text{ km}$, and $D_1^{\text{outside}} = 1120 \times 10^{0.4}\text{ft} = 0.85 \text{ km}$.

Taken together, we have that

$$\begin{aligned} P_f(\text{blast}|r) &= 0.85 \left[0.7 [P(\text{severe damage}|r, \text{concrete})P_f(\text{blast} \mid \text{severe damage, concrete}) \right. \\ &\quad \left. + P(\text{moderate damage}|r, \text{concrete})P_f(\text{blast} \mid \text{moderate damage, concrete})] \right. \\ &\quad \left. + 0.3 [P(\text{severe damage}|r, \text{S1})P_f(\text{blast} \mid \text{severe damage, S1}) \right. \\ &\quad \left. + P(\text{moderate damage}|r, \text{S1})P_f(\text{blast} \mid \text{moderate damage, S1})] \right] \\ &\quad + 0.15P_f(\text{blast}|r, \text{outside}), \end{aligned} \quad (11)$$

$$\begin{aligned}
P_i(\text{blast}|r) = & 0.85 \left[0.7 [P(\text{severe damage}|r, \text{concrete})P_i(\text{blast} | \text{severe damage, concrete}) \right. \\
& + P(\text{moderate damage}|r, \text{concrete})P_i(\text{blast} | \text{moderate damage, concrete})] \\
& + 0.3 [P(\text{severe damage}|r, \text{S1})P_i(\text{blast} | \text{severe damage, S1}) \\
& \left. + P(\text{moderate damage}|r, \text{S1})P_i(\text{blast} | \text{moderate damage, S1})] \right]. \quad (12)
\end{aligned}$$

These two functions are plotted in Fig. 1(a).

1.2 Thermal Effects

Heat accounts for 35% of the blast's energy. The goal of this subsection is to compute $P_f(\text{burn}|r)$ and $P_i(\text{burn}|r)$, which are the probabilities of dying or being seriously injured from the thermal effects at a distance r from the detonation. The thermal effect is measured by the thermal fluence Q , which is in units of calories per square centimeter (abbreviated by cal/cm²). The thermal fluence at a distance r km from a surface blast with yield Y is (see equation (7.96.2) in [2]) $Q(r) = \frac{25fYT}{\pi r^2}$, where f is the thermal partition ($f = 0.18$ for a surface blast, pg 319 in [2]) and the transmittance is $T = (1 + 1.9\frac{r}{v})e^{-2.9r/v}$ (pg 3-9 in [5]), where v is the visibility in km ($v = 19$ on a clear day). Hence, we have

$$Q(r) = \frac{1.43Y(1 + 1.9\frac{r}{v})e^{-2.9r/v}}{r^2}, \quad (13)$$

where $Y = 10$ kt and $v = 19$ km.

People can die or get injured from flash burns or from flame burns, i.e., directly from the thermal energy or indirectly from fires started by the thermal energy. We ignore any eye injuries: there were very few burned retinas at Hiroshima and flash blindness is only temporary ([2], pg 570). As in §1.1, we assume that 85% of the people are inside at the time of the blast, and 15% are outside. For people who are inside, their casualty probabilities depend on whether or not they are in a burned building. Hence, we consider three cases:

people who are inside burned buildings, people who are outside, and people who are inside buildings that are not burned.

We begin with people inside a burned building, and compute $P(\text{burned building}|r)$, which is the probability that a building a distance r from the detonation is burned. Fig. 5 of [6] shows that 90% of Hiroshima buildings burned at $Q = 48 \text{ cal/cm}^2$ and 50% burned at $Q = 11 \text{ cal/cm}^2$. For use in our setting (although Hiroshima's buildings may not reflect current U.S. buildings), we convert these Q values to $r = 0.54 \text{ km}$ and 1.1 km , respectively, via equation (13). We use these two distances to fit $P(\text{burned building}|r)$ to the complementary lognormal cdf,

$$P(\text{burned building}|r) = \frac{1}{2} - \frac{1}{2} \operatorname{erf} \left(\frac{\ln(r) - \alpha_{bb}}{\beta_{bb} \sqrt{2}} \right), \quad (14)$$

where

$$\alpha_{bb} = \ln(D_{50}^{bb}), \quad (15)$$

$$\beta_{bb} = \frac{\ln(D_{90}^{bb}) - \alpha_{bb}}{\sqrt{2} \operatorname{erf}^{-1}(-0.8)}, \quad (16)$$

with $D_{50}^{bb} = 1.1 \text{ km}$, $D_{90}^{bb} = 0.54 \text{ km}$.

We assume that the casualty probabilities inside a burned building are the same as the delayed casualties (i.e., thermal casualties because the immediate casualties are caused by the blast) inside a severely damaged concrete building in Table 12.21 of [2] (thereby assuming that the thermal injuries dominated prompt radiation injuries inside these buildings in Japan, which seems reasonable since this was an aerial detonation). Assuming that blast and burn events are statistically independent, we have

$$P_f(\text{blast or burn}) = P_f(\text{blast}) + P_f(\text{burn}) - P_f(\text{blast})P_f(\text{burn}). \quad (17)$$

Recalling that $P_f(\text{blast}) = 0.5P_f(\text{blast or burn}) = 0.44$ in Table 12.21 of [2], we can solve for $P_f(\text{burn}|\text{burned building}) = \frac{0.44}{1-0.44} = 0.79$. Using the same reasoning as in the calculation of the blast injury probability in a concrete building (i.e., assuming that the likelihood

of burn injury is independent of whether or not someone has previously died from blast effects, and that half of the injuries were due to burns), we have $P_i(\text{burn}|\text{burned building}) = \frac{0.11/2}{1-0.88}(1 - \frac{0.44}{1-0.44}) = 0.10$.

For people inside an unburned building or outside, casualties are caused directly by the thermal energy, and their casualty probabilities depend upon the exposed level of thermal energy at location r , denoted by $Q_{\text{exp}}(r)$. Because people are shielded by buildings (when both outside and inside), we typically have $Q_{\text{exp}}(r) \leq Q(r)$, and we set $Q_{\text{exp}}(r) = s_{Q_o}Q(r)$ for people who are outside at location r , and $Q_{\text{exp}}(r) = s_{Q_i}Q(r)$ for people who are inside a moderately-damaged building at location r , where s_{Q_o} and s_{Q_i} are outdoor and indoor thermal transmission factors, respectively; in our model, all severely-damaged buildings are burned, and we assume that people inside an undamaged building are fully protected from thermal energy.

Victims of direct thermal energy can receive first-degree (similar to bad sunburn), second-degree (blisters, infection and scars if untreated), or third-degree (skin and underlying tissue are destroyed) burns, depending upon the exposed level of thermal energy. In our casualty calculations, we ignore first-degree burns, assume second-degree burns are 50% fatal ([7], Fig. 1-3) and cause a thermal injury in the other 50%, and assume third-degree burns are 100% fatal (pg 220 of the 2003 version of [2] states that second- or third-degree burns over $\geq 20\%$ of the body requires hospitalization for successful recovery). That is, we assume that the casualty probabilities from direct thermal energy take the generic form

$$P_f(\text{burn}|r) = 0.5P(\text{second - degree burn}|Q_{\text{exp}}(r)) + P(\text{third - degree burn}|Q_{\text{exp}}(r)), \quad (18)$$

$$P_i(\text{burn}|r) = 0.5P(\text{second - degree burn}|Q_{\text{exp}}(r)). \quad (19)$$

We linearly interpolate using the data (based on people that are outside) in Fig. 12.65

in [2] to estimate the conditional probabilities on the right side of (18)-(19):

$$P(\text{second - degree burn}|Q_{\text{exp}}(r)) = \begin{cases} \max\{0, 0.18 + 0.32(Q_{\text{exp}}(r) - 3.5) & \text{if } Q_{\text{exp}}(r) \leq 4.5 \text{ cal/cm}^2; \\ 0.5 + \frac{0.32}{1.5}(Q_{\text{exp}}(r) - 4.5) & \text{if } Q_{\text{exp}}(r) \in (4.5, 6] \text{ cal/cm}^2; \\ 1 - P(\text{third - degree burn}|r) & \text{if } Q_{\text{exp}}(r) > 6 \text{ cal/cm}^2, \end{cases} \quad (20)$$

$$P(\text{third - degree burn}|Q_{\text{exp}}(r)) = \begin{cases} 0 & \text{if } Q_{\text{exp}}(r) \leq 5.4 \text{ cal/cm}^2; \\ 0.18 + \frac{0.32}{1.2}(Q_{\text{exp}}(r) - 6) & \text{if } Q_{\text{exp}}(r) \in (5.4, 7.2] \text{ cal/cm}^2; \\ \min\{1, 0.5 + \frac{0.32}{1.3}(Q_{\text{exp}}(r) - 7.2)\} & \text{if } Q_{\text{exp}}(r) > 7.2 \text{ cal/cm}^2. \end{cases} \quad (21)$$

Three tasks remain: the estimation of s_{Q_o} , s_{Q_i} , and the fraction of buildings at a distance r from the blast that are moderately damaged and not burned. Beginning with s_{Q_o} , we know that at Hiroshima, the distance at which half of the people outside died (i.e., the D_{50} in our notation) was 1.3 miles (page 546 in [2]), which corresponds to a thermal energy (unshielded by buildings) of 9 cal/cm² (Fig. 5 in [6]). Beyond this distance of 1.3 miles, there were essentially no burned buildings ([8], Fig. 3), no lethal prompt radiation ([2], Chapter 8), and not very many destroyed buildings ([8], Fig. 3). If we assume that the people outside at this distance died of flash burns, then we can use equations (18), (20) and (21) to determine that the value of $Q_{\text{exp}}(r)$ such that $P_f(\text{burn}|r) = 0.5$ is 5.76 cal/cm². Hence, we set $s_{Q_o} = \frac{5.76}{9} = 0.64$.

Assuming that blast and burn events are statistically independent, we have that the probability that a building at a distance r from the blast is moderately damaged and not burned is

$$P(\text{moderate damage, not burned}|r) = [0.7P(\text{moderate damage}|r, \text{concrete}) + 0.3P(\text{moderate damage}|r, S1)][1 - P(\text{burned building}|r)] \quad (22)$$

We could not find any data in [2], [5] or elsewhere to reliably estimate the indoor transmission factor for a moderately-damaged building, s_{Q_i} . Thermal energy travels through

windows, and we make the crude assumption that $s_{Q_i} = 0.2$, which accounts both for the transmission through windows and for the fact that some people are not near a window.

Combining these calculations, we have that the probability of death from thermal effects at a distance r from the blast is

$$\begin{aligned}
P_f(\text{burn}|r) = & 0.15[0.5P(\text{second - degree burn}|s_{Q_o}Q(r)) + P(\text{third - degree burn}|s_{Q_o}Q(r))] \\
& + 0.85P(\text{burned building}|r)P_f(\text{burn|burned building}) \\
& + 0.85P(\text{moderate damage, not burned}|r)[0.5P(\text{second - degree burn}|s_{Q_i}Q(r)) \\
& + P(\text{third - degree burn}|s_{Q_i}Q(r))], \tag{23}
\end{aligned}$$

where $s_{Q_o} = 0.64$, $s_{Q_i} = 0.2$, $P_f(\text{burn|burned building}) = \frac{44}{56}$, and the quantities $Q(r)$, $P(\text{burned building}|r)$, $P(\text{second - degree burn}|Q_{\text{exp}}(r))$, $P(\text{second - degree burn}|Q_{\text{exp}}(r))$ and $P(\text{moderate damage, not burned}|r)$ are defined in equations (13), (14), (20), (21) and (22), respectively.

Similarly, the probability of injury from thermal effects at a distance r from the blast is

$$\begin{aligned}
P_i(\text{burn}|r) = & 0.15[0.5P(\text{second - degree burn}|s_{Q_o}Q(r))] \\
& + 0.85P(\text{moderate damage, not burned}|r)[0.5P(\text{second - degree burn}|s_{Q_i}Q(r))] \\
& + 0.85P(\text{burned building}|r)P_i(\text{burn|burned building}), \tag{24}
\end{aligned}$$

where $P_i(\text{burn|burned building}) = 0.058$. The two functions in (23)-(24) are shown in Fig. 1(b).

1.3 Prompt Radiation

The goal of this subsection is to compute the fatality probability $P_f(\text{prompt}|r)$ and injury probability $P_i(\text{prompt}|r)$ at location r due to prompt radiation, which is – by definition –

emitted within the first minute, and represents 5% of the total energy. This radiation can be divided into three categories: neutrons, secondary gamma rays and fission product gamma rays. We will follow the approach described in Chapter 5 of [5]. Let $D_p^N(r)$ be the neutron radiation at a distance r (measured in yards) from the detonation. By page 5-26 of [5], this function can be expressed as $D_p^N(r) = \frac{Y F_N(0) e^{-\mu_N r}}{r^2}$, where the yield $Y = 10$ kt, and the constants $F_N(0)$ (which is in units of yards²· rad/kt) and μ_N depend on r and the type of weapon; we assume a gun-assembly fission weapon [1], which is weapon type VI in [5], and estimate these two constants from Figs. 5-9b and 5-10b in [5] (Table 1).

Similarly, the secondary gamma ray dose at location r is $D_p^{\gamma s}(r) = \frac{Y F_{\gamma s}(0) e^{-\mu_{\gamma s} r}}{r^2}$, where $\mu_{\gamma s}$ and $F_{\gamma s}(0)$ are estimated from Figs. 5-12b and 5-13b in [5] (Table 1).

By page 5-30 of [5], the fission product gamma ray dose can be expressed as $D_p^{\gamma f}(r) = Y H_r H_w E F_{\gamma f}(0) e^{-\mu_{\gamma f} r}$, where $H_w = 0.83$ (Fig. 5-16 of [5]) is the yield-dependent burst height adjustment factor, $E = 3$ (Fig. 5-17 in [5]) is the hydrodynamic enhancement factor, and H_r is the range-dependent burst height adjustment factor. We set H_r equal to a piecewise linear function between the three points $(r, H_r) = (500, 0.88), (1000, 0.95)$ and $(2000, 1)$, and equal to 1 otherwise (Fig. 5-15 in [5]). The constants $\mu_{\gamma f}$ and $F_{\gamma f}(0)$ (which is in units of rad/kt) are estimated from Fig. 5-14 in [5] (Table 1).

When adding radiation doses, one typically multiplies each dose by the relative biological effectiveness (RBE) of the radiation, which converts from rads to rems. However, for immediate radiation injury, the RBE for all three types of radiation equals 1, and so we can simply define the total prompt radiation at location r by

$$D_p(r) = D_p^N(r) + D_p^{\gamma s}(r) + D_p^{\gamma f}(r). \quad (25)$$

As in §1.2, we incorporate shielding by buildings. A person who is outside in a built-up urban setting may receive only 20-70% of the full radiation dose (pg. 441 of [2]). Because most buildings within 0.5 km will be immediately destroyed (and hence will not provide

radiation shielding), we assume that the outdoor dose transmission factor is $s_{Do}(r)$ is given by

$$s_{Do}(r) = \begin{cases} 1.0 & \text{if } r < 0.5 \text{ km;} \\ 0.45 & \text{if } r > 0.5 \text{ km,} \end{cases} \quad (26)$$

Dose transmission factors vary by building type, location within a building, and radiation type: e.g., it is 0.8-1.0 (gamma rays) and 0.3-0.8 (neutrons) for a frame house, and 0.3-0.6 (gamma rays) and 0.3-0.8 (neutrons) for the lower stories of a multistory apartment building (Table 8.72 in [2]); see Fig. 2 in [9] for how the transmission factor depends on the location within a large building. To capture this interperson heterogeneity, we let $s_{Di}(r)$ be a uniform random variable with mean $\bar{s}_{Di}(r)$ and range $[\bar{s}_{Di}(r) - 0.2, \bar{s}_{Di}(r) + 0.2]$ for $r \geq 0.5$ km; we again assume that buildings offer no protection for $r < 0.5$ km, so that $s_{Di}(r)$ takes on the value $\bar{s}_{Di}(r) = 1.0$ with probability one if $r < 0.5$ km. There are two counteracting forces at work: as r increases, buildings are less damaged (leading to more protection), but buildings are typically smaller (leading to less protection). We let $\bar{s}_{Di}(r)$ decrease linearly from 0.5 at $r = 0.5$ km to 0.3 at $r = 4$ km, which is the 0.6 psi threshold for broken windows ([1], pg 1-24):

$$\bar{s}_{Di}(r) = \begin{cases} 1.0 & \text{if } r < 0.5 \text{ km;} \\ \frac{3.7-0.4r}{7} & \text{if } r \in [0.5, 4] \text{ km;} \\ 0.3 & \text{if } r > 4 \text{ km.} \end{cases} \quad (27)$$

Equation (27) underestimates the transmission factors in an urban setting because many people will be in large buildings.

We estimate the probability of death or injury due to prompt radiation with generic dose D by the lognormal complementary cdfs,

$$P_f(D) = \frac{1}{2} - \frac{1}{2} \operatorname{erf} \left(\frac{\ln(D) - \alpha_{fp}}{\beta_{fp} \sqrt{2}} \right), \quad (28)$$

$$P_i(D) = \frac{1}{2} \operatorname{erf} \left(\frac{\ln(D) - \alpha_{fp}}{\beta_{fp} \sqrt{2}} \right) - \frac{1}{2} \operatorname{erf} \left(\frac{\ln(D) - \alpha_{ip}}{\beta_{ip} \sqrt{2}} \right), \quad (29)$$

where

$$\alpha_{fp} = \ln(D_{50}^{fp}), \quad (30)$$

$$\beta_{fp} = \frac{\ln(D_{90}^{fp}) - \alpha_{fp}}{\sqrt{2}\operatorname{erf}^{-1}(-0.8)}, \quad (31)$$

$$\alpha_{ip} = \ln(D_{50}^{ip}), \quad (32)$$

$$\beta_{ip} = \frac{\ln(D_{90}^{ip}) - \alpha_{ip}}{\sqrt{2}\operatorname{erf}^{-1}(-0.8)}. \quad (33)$$

Using dose-response data on page 1-26 of [1], taken from [5], we set $D_{50}^{fp}=385$ rem, $D_{90}^{fp}=500$ rem, $D_{50}^{ip}=215$ rem, and $D_{90}^{ip}=280$ rem.

Hence, we have

$$P_f(\text{prompt}|r) = 0.85P_f(s_{Di}(r)D_p(r)) + 0.15P_f(s_{Do}(r)D_p(r)), \quad (34)$$

$$P_i(\text{prompt}|r) = 0.85P_i(s_{Di}(r)D_p(r)) + 0.15P_i(s_{Do}(r)D_p(r)). \quad (35)$$

These two functions are depicted in Fig. 1(c).

1.4 Combined Effects

Although many victims suffer some combination of blast, burn and radiation injuries, the casualty functions for fatalities and injuries specified in §1.1-1.3 assume that people only suffer from one type of effect. In this subsection, we derive the overall fatality probability $P_f(r)$ and injury probability $P_i(r)$ in terms of the functions $P_f(\text{blast}|r)$, $P_f(\text{burn}|r)$, $P_f(\text{prompt}|r)$, $P_i(\text{blast}|r)$, $P_i(\text{burn}|r)$ and $P_i(\text{prompt}|r)$ given earlier.

The injury probabilities $P_i(\text{blast}|r)$, $P_i(\text{burn}|r)$ and $P_i(\text{prompt}|r)$ do not take into account the fact that these injuries may be precluded by death due to either of the other two injuries (although prompt radiation fatalities are delayed, we still need to account for them when calculating injuries). For ease of presentation, we define $P_i^*(\text{blast}|r)$, $P_i^*(\text{burn}|r)$ and

$P_i^*(\text{prompt}|r)$ to be the probability of injury due to one effect and not dying from either of the other two effects:

$$P_i^*(\text{blast}|r) = P_i(\text{blast}|r)[1 - P_f(\text{burn}|r) - P_f(\text{prompt}|r) + P_f(\text{burn}|r)P_f(\text{prompt}|r)], \quad (36)$$

$$P_i^*(\text{burn}|r) = P_i(\text{burn}|r)[1 - P_f(\text{blast}|r) - P_f(\text{prompt}|r) + P_f(\text{blast}|r)P_f(\text{prompt}|r)], \quad (37)$$

$$P_i^*(\text{prompt}|r) = P_i(\text{prompt}|r)[1 - P_f(\text{blast}|r) - P_f(\text{burn}|r) + P_f(\text{blast}|r)P_f(\text{burn}|r)]. \quad (38)$$

Animal studies and Japanese data show that the D_{50} value for radiation is significantly decreased in the presence of serious burn or blast injuries [7]. Table 3.1 in [7] estimates that the expectant radiation dose in the absence of other injuries is 4.5 Gy (where 1 rad = 0.01 Gy), and the expectant dose in the presence of a serious burn or blast injury is 1.5 Gy. Hence, we reduce the fatality fractiles by a factor of three if the person has either a burn or a blast injury (or both), yielding $\tilde{D}_{50}=128$ rem, and $\tilde{D}_{90}=167$ rem. We refer to the resulting lognormal complementary cdf as $\tilde{P}_f(D)$ and the resulting fatality probability in (34) as $\tilde{P}_f(\text{prompt}|r)$, and we assume that this probability applies for people who have a combined injury of radiation with blast and/or burns. Although combined blast-burn injuries lead to enhanced mortality, little quantitative data are available for this type of injury ([5], pg 10-33), and we arbitrarily assume that 30% of people with a combined blast-burn injury (where neither in isolation is fatal) die.

Taken together, we have that

$$\begin{aligned} P_f(r) = & 1 - [1 - P_f(\text{blast}|r)][1 - P_f(\text{burn}|r)][1 - P_f(\text{prompt}|r)] \\ & + [P_i^*(\text{blast}|r) + P_i^*(\text{burn}|r) - P_i^*(\text{blast}|r)P_i^*(\text{burn}|r)]\tilde{P}_f(\text{prompt}|r) \\ & + 0.3P_i^*(\text{blast}|r)P_i^*(\text{burn}|r)[1 - \tilde{P}_f(\text{prompt}|r)], \end{aligned} \quad (39)$$

$$\begin{aligned}
P_i(r) = & P_i^*(\text{blast}|r) + P_i^*(\text{burn}|r) + P_i^*(\text{prompt}|r) - P_i^*(\text{blast}|r)P_i^*(\text{burn}|r) \\
& - P_i^*(\text{blast}|r)P_i^*(\text{prompt}|r) - P_i^*(\text{burn}|r)P_i^*(\text{prompt}|r) \\
& + P_i^*(\text{blast}|r)P_i^*(\text{burn}|r)P_i^*(\text{prompt}|r) \\
& - [P_i^*(\text{blast}|r) + P_i^*(\text{burn}|r) - P_i^*(\text{blast}|r)P_i^*(\text{burn}|r)]\tilde{P}_f(\text{prompt}|r) \\
& - 0.3P_i^*(\text{blast}|r)P_i^*(\text{burn}|r)[1 - \tilde{P}_f(\text{prompt}|r)]. \tag{40}
\end{aligned}$$

The two functions in (39)-(40) are shown in Fig. 1(d). Note that the probability of injury in Fig. 1(d) initially increases with distance and then decreases with distance because death precludes injury until about 0.8 km from the detonation.

Recall that we are very uncertain about three parameter values: the mix of building types, the fraction of outside blast casualties that are fatalities, and the indoor thermal transmission factor, s_{Qi} . Changing the mix of concrete and S1 buildings from 70-30 to 30-70 causes virtually no change in our casualty figures, because the blast effects are largely subsumed by prompt radiation effects for $r < 1$ km and by burn effects for $r > 1$ km. Similarly, allowing half of the outside blast fatalities in equation (9) to be blast injuries has a very minor impact, for the reasons stated above and because only 15% of people are outside. Finally, changing s_{Qi} from its base-case value of 0.2 to 0.5 again has virtually no change in casualty: increasing the number of prompt fatalities by 0.1% and increasing the number of prompt injuries by 1.0%.

Our results are qualitatively similar to those in [1] and [10], which also consider a 10-kt blast in Washington D.C. Although burn casualties are not explicitly considered in [1], information in Table 1-7 of [1] are consistent with our burn casualties in Fig. 1(b), and our prompt casualties in Fig. 1(c) are consistent with information in Table 1-15 of [1]. The main difference is that we have less blast injuries than in [1], perhaps because we estimate these using data in [2, 5] for serious injuries (i.e., injuries requiring hospitalization).

1.5 Spatial Distribution of the Population

Because the detonation occurs at 10 am on a weekday, we need the spatial distribution of the daytime population in Washington DC and its surrounding areas. We obtain the spatial distribution of the nighttime population within 160 km of the Washington Mall (which is the origin in our spatial model, and is located at 38.89° latitude and -77.05° longitude) from LandScan USA [11], where the cell size is 0.721×0.928 km². There are 627,176 people within $r < 7.1$ km (which roughly corresponds to Washington D.C.) and 398,112 people within $r < 5$ km. To obtain the spatial distribution of the daytime population, we follow [1] and add 481k people uniformly to the region $r < 5$ km (or 4087 per cell) and add 220k uniformly to the annulus between $r = 5$ and 11 km (or 477 people per cell), bringing the total population in this annulus to 941,213.

The resulting spatial distribution gives us $n(x, y)$, which is the number of people per km² located at location (x, y) at the time of the blast. For the purposes of our model, we need to partition $n(x, y)$ into three groups: those people who die from prompt effects, the survivors of the prompt effects who incur a burn and/or blast injury (and hence whose total prompt plus fallout radiation dose is subject to the fatal dose-response function $\tilde{P}_f(D)$), and those survivors who incur neither a burn nor a blast injury (whose total radiation dose is subject to the fatal dose-response function $P_f(D)$).

The number of people in the first group is $P_f(r)n(x, y)$, where r and (x, y) are related via $r = \sqrt{x^2 + y^2}$. The number of people in the third group are the survivors who are either uninjured or incur only a prompt radiation injury, and hence is given by $P_u(r)n(x, y)$, where

$$P_u(r) = 1 - P_f(r) - P_i(r) + P_i^*(\text{prompt}|r)[1 - P_i^*(\text{blast}|r)][1 - P_i^*(\text{burn}|r)]. \quad (41)$$

Consequently, the number of people in the second group is $[1 - P_f(r) - P_u(r)]n(x, y)$.

2 Radiation Fallout

The residual (i.e., > 1 min) radiation (from fission daughter products, which is 10% of the total energy) is called fallout, and is differentiated into early (< 24 hr) fallout and late (> 24 hr) fallout, with a little over half of the fallout being early [2] ([1] assumes 55% of the fallout is early). Early fallout particles tend to be rather large (0.01-1 μ m, which is too large to inhale), and early fallout is dominated by external whole-body gamma radiation from the ground and – to a lesser extent – external beta radiation on the skin (pg 442 of [2]). Late fallout has smaller particles and causes mostly internal exposure via inhalation or ingestion of the smaller alpha and beta particles; $\approx 50\%$ of the inhaled particles end up in the GI system within hours [7]. Beta and alpha radiation are very low energy and cannot pass through skin or clothing. The biologically equivalent dose is measured in rem (or Sv, where $1 \text{ Sv} = 100 \text{ rem}$), and is the absorbed dose (in Gy) times the Relative Biological Effectiveness (RBE) for the particular radiation absorbed. The RBE for gamma and beta radiation is ≈ 1 , as is acute neutron radiation, whereas the RBE of delayed-injury neutron is 4-10 and the RBE of alpha radiation is 10-20 (page 577 of [2]). In our model, we assume the RBE of the fallout is 1.

The fallout is not spatially symmetric, and depends on the wind speed ($\nu = 10$ mph) and direction. For ease of exposition, we assume that the coordinate system is such that the wind direction is along the positive x axis. Our goal in this section is to determine the fallout dose rate $D_f(x, y, t)$ at location (x, y) at time t . We use [12], which constructs a relatively simple equation for $D_f(x, y, t)$ that has been calibrated against the more complicated NARAC model [13]. The equation in [12] is

$$D_f(x, y, t) = \frac{Y_0 t^{-1.2} [A e^{-\left(\frac{y}{\sigma}\right)^2} + (1 - A) e^{-\left[\frac{y}{\Delta} + \left(\frac{y}{\sigma}\right)^4\right]}]}{(a + x)^b [1 + e^{-\frac{(t-t_A)}{\sigma}}]}, \quad (42)$$

which is in units of rads/hr (or rems/hr, since we are assuming that $\text{RBE} = 1$).

The remainder of this section specifies the parameter values in equation (42). We start with the $\frac{Y_0}{(a+x)^b}$ term, which measures the spatial distribution along the wind direction (i.e., the plume length). We assume that $a = 2.5$ [12], independent of windspeed. We use Table II in [12] to construct two equations in terms of two unknowns, and derive $b = 1.7$ and $Y_0 = 1.75 \times 10^4$ for $\nu = 15$ mph. We linearly interpolate between these values and the values $Y_0 = 3.59 \times 10^4$ and $b = 1.9$ for the $\nu = 5$ mph case [12] to get $Y_0 = 2.67 \times 10^4$ and $b = 1.8$ for our $\nu = 10$ mph setting.

In the time-dependent part of (42), $\frac{t^{-1.2}}{1+e^{-\frac{(t-t_A)}{\sigma}}}$, the $t^{-1.2}$ power law is well established ([2], pg 391), $t_A = \frac{x}{\nu}$ is the arrival time of the plume, and $\sigma = 0.0016x + 0.0087$, which is derived by fitting a linear function $\sigma(x)$ for the $\nu = 15$ mph data in Table II of [12] as is already done there for the $\nu = 5$ mph data in Table I of [12], and then linearly interpolating between these two cases.

The final term in (42), $Ae^{-\left(\frac{y}{\delta}\right)^2} + (1-A)e^{-\left[\frac{y}{\Delta} + \left(\frac{y}{c}\right)^4\right]}$, specifies the spatial distribution perpendicular to the wind direction (i.e., the plume width). The five parameters in this expression depend upon the downwind distance x and Table 2 contains values of the parameters for three different distances [14]. We fit piecewise-linear functions to these values and obtain $\delta(x) = 0.044x + 0.26$, $\Delta = 3.8$,

$$A(x) = \begin{cases} -0.01x + 0.98 & \text{for } x \in [0, 10] \text{ km;} \\ 0.88 & \text{for } x > 10 \text{ km,} \end{cases} \quad (43)$$

$$c(x) = \begin{cases} 0.04x + 2.1 & \text{for } x \in [0, 10] \text{ km;} \\ 0.1x + 1.5 & \text{for } x > 10 \text{ km.} \end{cases} \quad (44)$$

3 Self-evacuation

In this section, we describe the model for self-evacuation. The time delay until evacuation begins is described in §3.1, and the models for evacuation by foot and by vehicle are given

in §3.2 and §3.3, respectively. Deaths due to radiation fallout are computed in §3.4.

3.1 Loading Time

Those who evacuate from a distance r from the blast do so after a time delay (sometimes called the loading time) that is the sum of two parts: a diffusion time until they learn about the event, and a preparation time, which is the delay from when they learn about the event until they begin to evacuate. The diffusion time is essentially zero (although some Japanese survivors had temporary acute anxiety, leading to impulsive and maladaptive behavior right after the detonation [15]) for $r < r_p$, where r_p certainly includes the distance where moderate blast damage occurs (e.g., windows break at 0.6 psi, which corresponds to 4 km); even at this distance, the nature of the event may not be obvious to everyone. The mushroom cloud is visible for 1 hr ([2], pg 32), and so if visibility is 19 km (a clear day), then r_p could be significantly larger, depending upon how people process the event. We consider two values, $r_p = 4$ km and 17 km, which correspond to low and high personal situational awareness, respectively.

For $r \in [r_p, r_i]$, we assume that there are no electronic communications (telephones, television, Internet) among the general public (or from the government to the public). There is some divergence about the value of r_i : electricity is assumed to be restored outside of the fallout zone within 48 hr ([16], pg 31) and electricity and other services are assumed to be disrupted across much of the affected area for 10-20 days ([1], pg 1-4), while most media is assumed to be up and transmitting outside of the blast zone ([17], pg 11). More specifically, for a 10-kt surface blast, it is estimated in Table 1-15 of [1] that electric power would be out for at least one week for $r < 14$ km and likely be out for $r < 17$ km, and maybe be out for $r < 320$ km, and telecommunications would be out for at least one week for $r < 17$ km and likely be out for < 320 km. We consider two values, $r_i = 17$ km and 320 km, which

correspond to high and low interpersonal situational awareness, respectively. For $r > r_i$, we assume communications are intact; note that even in areas where the telephone system is operational, it is likely to be overloaded [16].

We assume that the precise location of the detonation is determined by a GPS satellite within 5 minutes [16] and that within 15 minutes this information is being broadcast by the media. We assume that people at $r > r_i$ will have a mean diffusion time of 1 hr (consistent with diffusion times from nearby industrial accidents [18, 19]). People located in $[r_p, r_i]$ will have to rely on battery-powered radios, face-to-face contact with neighbors, non-electronic communications with the government (e.g., loudspeakers atop vehicles [1]), or family members driving home with the news. We assume that the mean diffusion time here is 3 hr. The mean preparation time is likely to be minimal: while it has been estimated at 40 min for hurricanes, it has been ≈ 5 min for nearby chemical spills [20]. While some people – particularly in areas with poor communications – may delay the evacuation decision until they gain more confidence in the information [21], we assume the preparation time is 15 min for everyone. Hence, we let the loading time (in hr) be

$$\tau_l(r) = \begin{cases} 0.25 & \text{if } r < r_p \text{ km;} \\ 3.25 & \text{if } r \in [r_p, r_i) \text{ km;} \\ 1.25 & \text{if } r \geq r_i \text{ km,} \end{cases} \quad (45)$$

where we consider four scenarios (with $r_p=4$ or 17 km, and $r_i = 17$ or 320 km, depending upon whether personal and interpersonal situational awareness are high or low.

We assume that 85% of people are inside and 15% of people are outside during the diffusion time, and everyone is indoors during the 0.25 hr of preparation time.

3.2 Self-evacuation by Foot

Survivors can self-evacuate either by foot or by vehicle. To evacuate by vehicle, someone needs to own a vehicle (or have a friend or neighbor drive them), have the vehicle be in

operational condition after the detonation, and be in a location where the roads are passable. Many tourists and 39% of commuters will be without a vehicle [22], and 37% of Washington DC (i.e., $r < 7.1$ km) households do not own a car [23]; we assume that 38% of people in $r < 7.1$ km do not have access to a car, and that this fraction is linearly decreasing in r from 0.76 at $r = 0$ to 0 at $r = 7.1$ km.

In addition, vehicles need to survive the prompt effects of the detonation. Automobiles appear to be robust to blasts: although battered, they are still operational after being subjected to 5 psi ([2], pg 191). Automobiles catch on fire from secondary fires, not from direct thermal radiation ([2], §14-10), and so we assume vehicles do not catch on fire outside of the burn zone. We assume that the roads are passable for $r > r_0$, where r_0 is the maximum distance where either 30% of buildings are burned or 10% of buildings (using the 70-30 mix of concrete and type S1 buildings) are severely damaged:

$$\begin{aligned} r_0 &= \max\left\{\{r|P(\text{severe damage}|r) = 0.1\}, \{r|P(\text{burned building}|r) = 0.3\}\right\}, \\ &= \max\{1.3, 1.5\} = 1.5 \text{ km}. \end{aligned} \tag{46}$$

Hence, we assume that a fraction $P_v(r)$ of people have access (e.g., they or a friend or relative own one) to an evacuating vehicle at location r , where

$$P_v(r) = \begin{cases} 0 & \text{if } r < 1.5 \text{ km;} \\ 0.24 + \frac{0.76}{7.1}r & \text{if } r \in [1.5, 7.1] \text{ km;} \\ 1.0 & \text{if } r > 7.1 \text{ km.} \end{cases} \tag{47}$$

Depending upon the particular self-evacuation strategy, we assume that a fraction $P_{ev}(x, y)$ of survivors who have access to a vehicle at location (x, y) self-evacuate, and a fraction $1 - P_{ev}(x, y)$ shelter in place, and a fraction $P_{ef}(x, y)$ of survivors who do not have access to a vehicle at location (x, y) self-evacuate, and a fraction $1 - P_{ef}(x, y)$ shelter in place. Hence, the number of people per km^2 who evacuate by foot from location (x, y) is $[1 - P_f(r)][1 - P_v(r)]P_{ef}(x, y)n(x, y)$.

People who evacuate from location (x, y) by foot are assumed to move at 1 mph in a random direction that is uniformly distributed in $[\arctan(\frac{y}{x}) - \frac{\pi}{4}, \arctan(\frac{y}{x}) + \frac{\pi}{4}]$. Both the slow speed and the random direction incorporates the initial confusion about the location of the blast and the fact that people will need to move around buildings (and, for small r , through rubble), may be carrying things (including children), and may be injured. We assume that there are no congestion effects among pedestrians and no congestion interactions between pedestrians and vehicles (i.e., neither are slowed down by the other). Note that there is a very small group of people who die due to prompt radiation alone; these people typically live for at least several days and so may attempt to evacuate by foot. But because they will all be in $r < 1.5$ km (see Fig. 1(c)), and because we assume no congestion effects among pedestrians or between pedestrians and vehicles, by equation (47) we can safely ignore their evacuation efforts.

3.3 Self-evacuation by Vehicle

We assume that there are 2.5 people per evacuating vehicle [24]. Hence, the number of vehicles per km^2 that are evacuating (x, y) (given an evacuation strategy specified by $P_{ev}(x, y)$; several strategies are described in the main text) is

$$c(x, y) = \frac{[1 - P_f(r)]P_v(r)P_{ev}(x, y)n(x, y)}{2.5}. \quad (48)$$

For those evacuating by vehicle, we assume (as in [25]) they travel only via arcs (paths of constant radius from $(x, y) = (0, 0)$) and rays (paths emanating out from $(x, y) = (0, 0)$). Washington DC has approximately eight major evacuation routes out of the Beltway [26], and we assume that they are at angles $\phi + j\frac{\pi}{4}$ for $j = 0, 1, \dots, 7$, where ϕ is the angle between the wind direction and the first evacuation route. Because we anticipate vehicle congestion on the rays, we expect that casualties will be maximized when $\phi = 0$ (i.e., the fallout is centered on a ray) and minimized when $\phi = \frac{\pi}{8}$. Hence, in the base case, we set $\phi = \frac{\pi}{16}$.

Each ray is assumed to have four lanes in the outbound direction (we do not model the inbound direction). As a separate back-of-the-envelope calculation to assess the feasibility of this assumption, we know that during a typical evening rush hour, most of the outgoing routes from Washington D.C. are overloaded by at least 20% [27]. If we assume the 8 arcs have 4 lanes each, then the maximum capacity is 64k/hr (Fig. 3-3 of [28]). Among the 671.7k people employed in Washington D.C., 72% commute from outside the city, and among these, 39% use public transportation, 38% drive alone, and hence $\approx 23\%$ drive together [29]. Hence, roughly 236k vehicles are commuting out of town every evening; this corresponds to $236/64=3.7$ hr of flow on the rays, which seem reasonable.

We assume there are arcs every 3 km starting at $r_0 = 1.5$ km. Let the arc with radius $r_j = r_o + 3j$ be denoted by arc j for $j = 0, 1, \dots$. Each arc has two lanes of traffic moving in each direction. Let $\theta = \arctan(\frac{y}{x})$, so that a location can be specified by (x, y) or (r, θ) . All evacuating vehicles travel instantaneously at time $\tau_l(r)$ in the radial direction to the closest arc (i.e., from (r, θ) to (r_{j^*}, θ) , where $j^* = \arg \min_j |r - r_j|$; we ignore this travel time because it is a distance of at most 1.5 km), then travel along this arc to one of the two closest of the eight rays, and then travel outward on this ray until they are out of the fallout region. We call this the *shortest* evacuation procedure. At the end of this subsection, we also consider an *avoidance* evacuation procedure, where people travel along an arc to the closest ray that is not in the fallout zone. For a one-time emergency evacuation, it has been found empirically that most people use a predetermined evacuation route rather than the shortest route [20].

Consider location (r_j, θ) on arc j . The number of vehicles per km entering arc j at this location can be found by integrating $c(x, y)$ in (48) along the line segment containing (r_j, θ) and in the radial direction from $r_j - 1.5$ to $r_j + 1.5$: $\int_{r_j-1.5}^{r_j+1.5} c(r, \theta) dr$.

It has been estimated that local traffic during an evacuation increases by at least 50% due to household consolidation behavior (e.g., parents picking up children from school)

during an evacuation [30]. To model this in the simplest way, we assume that – irrespective of location – $\frac{3}{4}$ of vehicles travel to the closest ray and the remaining vehicles travel to the other adjacent ray, which leads to a 50% increase in aggregate distance traveled relative to the case in which each vehicle moved to the closest ray (i.e., if the distance between rays is d and drivers arrived randomly along this segment, then the average distance to the closest ray is $\frac{d}{4}$ and the average distance to the other adjacent ray is $\frac{3d}{4}$; hence, if $\frac{1}{4}$ of vehicles travel to the farther ray, then the average distance traveled is $\frac{3d}{8}$, which is 50% greater than $\frac{d}{4}$).

Traffic flow along arcs and rays is modeled according to a generalization (allowing for entrances and exits) of the classic kinematic wave model of Lighthill and Whitham [31], incorporating traffic engineering data from [28]. The kinematic wave model measures the velocity $v(s, t)$, the density $\rho(s, t)$ and the flow $q(s, t)$ along location s of a single-lane road at time t , where $q(s, t) = v(s, t)\rho(s, t)$. This model can be summarized by a single partial differential equation (PDE) using the conservation of mass equation and a specified relationship (based on traffic engineering data) between flow and density, which is $q = Q(\rho)$. The conservation of mass equation, which specifies that the increase in density at location s during a short interval near time t is equal to the inflow minus the outflow at location s at time t , is given by $\frac{\partial \rho(s, t)}{\partial t} + \frac{\partial q(s, t)}{\partial s} = 0$. Noting that $\frac{\partial q(s, t)}{\partial s} = \frac{dQ(\rho)}{d\rho} \frac{\partial \rho(s, t)}{\partial s}$, the conservation of mass equation can be written as $\frac{\partial \rho(s, t)}{\partial t} + \frac{dQ(\rho)}{d\rho} \frac{\partial \rho(s, t)}{\partial s} = 0$. As noted in §83 of [32], if we let $\beta(s, t)$ be the net (i.e., entering minus exiting) number of vehicles per hour entering the highway per km of roadway, then the PDE is

$$\frac{\partial \rho(s, t)}{\partial t} + \frac{dQ(\rho)}{d\rho} \frac{\partial \rho(s, t)}{\partial s} = \beta(s, t). \quad (49)$$

Before showing how to apply (49) to arc segments and rays, we specify the flow-density relationship $Q(\rho)$, which differs for arcs and rays. Fig. 3-3 of [28] provides this relationship for various speed limit designs (i.e., the speed in the absence of congestion) of 50, 60 and 70 mph (flow and density are given on a per lane basis in this figure). Although some

roads may close to secure key officials ([23], pg 16), and some researchers assume that roads only operate at 80% of their nominal capacity to account for accidents, vehicles running out of gas, etc. [33], we use the nominal capacities in [28]. We use the 50 mph curve for the arcs, which have two lanes, but we convert the units from miles to km. For a single lane, Fig. 3-3 of [28] suggests that $Q(0) = 0$, the flow is convex in density, and achieves its maximum at $Q(37.1) = 1900$ vehicles/hr. Moreover, Fig. 1-1 of [28] shows that this relationship is symmetric about $\rho = 37.1$ vehicles/km, implying that $Q(74.2) = 0$. We make two changes to this function: we double the flow and density because there are two lanes, and to incorporate traffic lights, we multiply the flow by 0.4 (assuming that this road has green lights 40% of the time - even if the traffic lights are inoperable after the detonation, interference from cross-traffic will remain); this latter modification is consistent with [33], which assumes the capacity (i.e., maximum flow) is the standard capacity times the fraction of time the lights are green. Incorporating both changes, fitting $Q(0) = 0$, $Q(74.2) = 1520$ and the intermediate point $Q(49.7) = 1256$ to a quadratic function, and imposing symmetry around $\rho = 74.2$ yields

$$Q_{\text{arc}}(\rho) = \begin{cases} 34.97\rho - 0.195\rho^2 & \text{for } \rho < 74.2; \\ 34.97(\rho + 34.93) - 0.195(\rho + 34.93)^2 & \rho \in [74.2, 148.4]. \end{cases} \quad (50)$$

For rays, we use the 70 mph curve in Fig. 3-3 of [28], multiply the flow and density by four, and fit $Q(0) = 0$, $Q(166.5) = 8000$ and $Q(24.9) = 2400$ to obtain

$$Q_{\text{ray}}(\rho) = \begin{cases} 105.1\rho - 0.342\rho^2 & \text{for } \rho < 166.5; \\ 105.1(\rho - 26.22) - 0.342(\rho - 26.22)^2 & \rho \in [166.5, 333]. \end{cases} \quad (51)$$

To apply (49) on arc segments, we need two versions of this PDE, one corresponding to each direction (clockwise and counterclockwise). Without loss of generality, we provide details only for the segment of arc j from ϕ to $\phi + \frac{\pi}{4}$ with the traffic flowing in the counterclockwise direction (from ϕ to $\phi + \frac{\pi}{4}$). The length of this arc segment is $\frac{\pi r_j}{4}$ and we denote the one-dimensional space index of this arc segment by the variable $s \in [r_j\phi, r_j(\phi + \frac{\pi}{4})]$. To fully

specify the PDE, we need to give the boundary conditions and the inflow and outflow rates on the right side of (49). For simplicity, we assume that the roads are empty at $t = 0$, so that $\rho(s, 0) = 0 \forall s$; this assumption is conservative with respect to our policy recommendation because it underestimates congestion and favors evacuation. In addition, because vehicles are not traveling from the ray at ϕ to the arc, we set $\rho(\phi, t) = 0 \forall t$.

Because the right side of (49) is the inflow minus the outflow, we denote it by $\beta_i^{\text{arc}}(s, t) - \beta_o^{\text{arc}}(s, t)$. These functions are dictated by downstream congestion. To estimate the inflow terms, we develop a queueing model for the vehicles waiting to get onto each location s of arc j . Recalling that $\frac{3}{4}$ of vehicles go to the closest ray and $\frac{1}{4}$ go the other ray, the number of vehicles per km arriving to the queue at location s of arc j at time t is

$$a_j(r_j\theta, t) = \begin{cases} \frac{1}{4} \int_{r_j-1.5}^{r_j+1.5} c(r, \theta) dr & \text{if } t = \tau_l(r_j) \text{ km}, \theta \in [\phi, \phi + \frac{\pi}{8}); \\ \frac{3}{4} \int_{r_j-1.5}^{r_j+1.5} c(r, \theta) dr & \text{if } t = \tau_l(r_j) \text{ km}, \theta \in [\phi + \frac{\pi}{8}, \phi + \frac{\pi}{4}]; \\ 0 & \text{otherwise.} \end{cases} \quad (52)$$

Let $A_j(s, t) = \int_0^t a_j(s, t) dt$ be the cumulative number of vehicle arrivals per km at location s up to time t .

In our queueing model, vehicles wait to get onto an arc in a first-come first-served fashion until there is available space, which is determined by the vehicle density $\rho(s, t)$, and vehicles that enter the arc correspond to service completions in the queue. We know from our calculation of $Q(\rho)$ that the maximum density of vehicles on the two-lane arc is 148.4 vehicles/km. Assuming that vehicles in the queue are merging onto the arc in only one of the two lanes (i.e., the right line), we let the potential service rate $\mu_{\text{arc}}(s, t)$ (in vehicles/km) be one-half of the excess capacity:

$$\mu_{\text{arc}}(s, t) = \frac{1}{2}(148.4 - \rho(s, t)). \quad (53)$$

The potential service rate may differ from the actual service rate if there are not sufficient vehicles in queue. That is, the density of vehicles entering the arc is the minimum of the

density of vehicles waiting to enter the arc and the potential service rate in (53), which represents the available density on the arc. To understand the dynamics of merging onto the arcs, suppose the density $\rho(s, t) = 0$ for a particular location s and time t , so that the slack capacity in (53) is 74.2 vehicles/km. Now assume that a large bulk arrival of vehicles occurs at time $\tau_l(r)$ at location s . Then at the next time interval of the computer program, 74.2 vehicles/km enter the arc in the right lane. Instantaneously, half of these vehicles move into the left lane, which was previously empty, and the two-lane arc is loaded to half of its capacity. In the next time interval of the computer program, the slack capacity $\mu_{\text{arc}}(s, t)$ is cut in half, to $0.5(148.4-74.2)$. Now we allow 37.1 vehicles/km onto the arc, which loads the arc to roughly $\frac{3}{4}$ of its capacity (assuming there is still a big queue of vehicles waiting to enter the arc). In this manner, over the subsequent time intervals the arc density increases to approximately $\frac{7}{8}$, $\frac{15}{16}$, etc. of its maximum density; i.e., the arc will become fully loaded and vehicles will wait longer in the queue.

Let $S(s, t) = \int_0^t \mu_{\text{arc}}(s, t) dt$ be the cumulative number of potential service completions per km at location s up to time t . Then the queue length of vehicles per km at location s at time t is given by [34]

$$L(s, t) = A_j(s, t) - S(s, t) - \inf_{0 \leq u \leq t} \{A_j(s, u) - S(s, u)\}. \quad (54)$$

Moreover, the cumulative number of service completions per km at location s up to time t is $S(s, t) + \inf_{0 \leq u \leq t} \{A_j(s, u) - S(s, u)\}$ [34]. Because a service completion in the queue corresponds to a vehicle entering an arc, the inflow rate $\beta_i^{\text{arc}}(s, t)$ satisfies

$$\int_0^t \beta_i^{\text{arc}}(s, u) du = S(s, t) + \inf_{0 \leq u \leq t} \{A_j(s, u) - S(s, u)\}. \quad (55)$$

The only departures from the arc segment occur at the arc-ray intersection, and hence $\beta_o^{\text{arc}}(s, t) = 0$ for $s \in [\phi, \phi + \frac{\pi}{4})$. These arc departures correspond to ray arrivals. Following equation (1b) of [35], we assume that the density of vehicles exiting the arc segment to the

ray is the minimum of three quantities: the density of vehicles wishing to exit the arc (i.e., $\rho_{\text{arc}}(\phi + \frac{\pi}{4}, t)$), the capacity out of the arc (only one lane exits the arc to the ray, and so this is equal to one-half of the arc's maximum density, i.e., $\frac{1}{2}(148.4)$), and the available density in the right lane on the ray at $r = r_j$ (which is one-quarter of the ray's excess density, i.e., $\frac{1}{4}(333 - \rho_{\text{ray}}(r_j, t))$). However, we need to keep in mind that traffic from two arcs is merging into the right lane of the ray at $(\phi + \frac{\pi}{4}, r_j)$: the counterclockwise traffic that we are describing in detail, and the clockwise traffic on the arc segment $r \in [r_j(\phi + \frac{\pi}{4}, r_j(\phi + \frac{\pi}{2})]$. Moreover, we assume that these two streams of traffic share the lane that exits from the arc to the ray. Let the density of clockwise traffic at the end of the arc segment $r \in [r_j(\phi + \frac{\pi}{4}, r_j(\phi + \frac{\pi}{2})]$ be denoted by $\tilde{\rho}_{\text{arc}}(\phi + \frac{\pi}{4}, t)$. Then $\beta_o^{\text{arc}}(\phi + \frac{\pi}{4}, t)$ satisfies

$$\beta_o^{\text{arc}}(\phi + \frac{\pi}{4}, t)\Delta t = \begin{cases} \rho_{\text{arc}}(\phi + \frac{\pi}{4}, t) & \text{if } \rho_{\text{arc}}(\phi + \frac{\pi}{4}, t) + \tilde{\rho}_{\text{arc}}(\phi + \frac{\pi}{4}, t) < \min\{\frac{1}{2}(148.4), \frac{1}{4}(333 - \rho_{\text{ray}}(r_j, t))\}; \\ \frac{\min\{\frac{1}{2}(148.4), \frac{1}{4}(333 - \rho_{\text{ray}}(r_j, t))\}}{2} & \text{if } \min\{\rho_{\text{arc}}(\phi + \frac{\pi}{4}, t), \tilde{\rho}_{\text{arc}}(\phi + \frac{\pi}{4}, t)\} > \frac{\min\{\frac{1}{2}(148.4), \frac{1}{4}(333 - \rho_{\text{ray}}(r_j, t))\}}{2}. \end{cases} \quad (56)$$

The conditions in (56) correspond to either both exiting arc flows or neither exiting arc flow being fully accommodated. If neither condition in (56) holds, then one of the two exiting arc flows can be fully accommodated, and

$$\beta_o^{\text{arc}}(\phi + \frac{\pi}{4}, t)\Delta t = \begin{cases} \rho_{\text{arc}}(\phi + \frac{\pi}{4}, t) & \text{if } \rho_{\text{arc}}(\phi + \frac{\pi}{4}, t) < \tilde{\rho}_{\text{arc}}(\phi + \frac{\pi}{4}, t); \\ \min\{\frac{1}{2}(148.4), \frac{1}{4}(333 - \rho_{\text{ray}}(r_j, t))\} - \tilde{\rho}_{\text{arc}}(\phi + \frac{\pi}{4}, t) & \text{if } \rho_{\text{arc}}(\phi + \frac{\pi}{4}, t) > \tilde{\rho}_{\text{arc}}(\phi + \frac{\pi}{4}, t). \end{cases} \quad (57)$$

Turning to the PDE for the rays, without loss of generality we describe the details for the ray at angle ϕ , and let the spatial variable of the PDE be the radial distance r . We assume that the roads are empty at $t = 0$, so that $\rho(r, 0) = 0 \forall r$. We define the right side of (49) by $\beta_i^{\text{ray}}(r, t) - \beta_o^{\text{ray}}(r, t)$. The inflows to the ray are due to departures from the arcs, and hence $\beta_i^{\text{ray}}(r, t) = 0$ for $r \neq r_j$ for some $j = 0, 1, \dots$. At location r_j on the ray, $\beta_i^{\text{ray}}(r_j, t)$

includes two source terms that correspond to (56)-(57): one term is the arc departures from counterclockwise traffic on the arc segment $s \in [r_j(\phi - \frac{\pi}{4}), r_j\phi]$ and the other is the arc departures from clockwise traffic on the arc segment $r \in [r_j\phi, r_j(\phi + \frac{\pi}{4})]$.

The outflow from the ray corresponds to vehicles that eventually exit the ray after leaving the fallout zone. We let r_e be the location of the outer edge of the fallout zone, which is defined to be the location such that the cumulative fallout over the first 96 hours is equal to $D_{10}^{ip} = 150$ rems (i.e., the value that causes radiation injury in 10% of the population): $r_e = \{x | \int_0^{96\text{hr}} D_f(x, 0, t) dt = 150\}$. Solving this equation gives 27.1 km, and we round this value to the closest arc location, $r_e = 27$ km. Our model extends out to $r_e + 90 = 117$ km, and we impose a Neumann (i.e., smooth) boundary condition at $r_e + 90$ km, which is $\frac{\partial \rho(r, t)}{\partial r} = 0$ at $r = r_e + 90$ km. We assume that there are no ray departures for $r < r_e$ and that $\frac{1}{30}$ of the ray density exits at each arc over the next 90 km, so that

$$\beta_o^{\text{ray}}(r_j, t)\Delta t = \begin{cases} \frac{\rho(r_j, t)}{30} & \text{for } r_j \in [r_e, r_e + 90) \text{ km;} \\ 0 & \text{otherwise.} \end{cases} \quad (58)$$

Note that these ray departures are not incorporated into the arc PDEs as arc arrivals. These ray departures occur very far from the detonation (where congestion should not be a major problem), and a small fraction of vehicles exit at each of these arcs.

We complete this subsection by describing how the avoidance evacuation model differs from the shortest evacuation model. The same basic model, equation (49), is used. For arc evacuation, we assume that every vehicle travels on the arc in the direction away from the centerline of the fallout plume. Hence, we need to model the arc flow in only one direction and there is not a 50% increase in local travel distance due to family consolidation. Moreover, there is no merger of flows at the arc-ray intersection, and equations (56)-(57) reduce to

$$\beta_o^{\text{arc}}(\phi + \frac{\pi}{4}, t)\Delta t = \min\{\rho_{\text{arc}}(\phi + \frac{\pi}{4}, t), \frac{1}{2}(148.4), \frac{1}{4}(333 - \rho_{\text{ray}}(r_j, t))\}. \quad (59)$$

3.4 Fallout Casualties

The solution to our evacuation model generates the spatiotemporal vehicle densities in (49) for the various arcs and rays. The specified relationship $q(s, t) = Q(\rho(s, t))$ gives us the flows, and the equation $v(s, t) = \frac{q(s, t)}{\rho(s, t)}$ provides us with the velocities. These velocities allow us to reconstruct the trajectory of every vehicle that evacuated from every location (x, y) at time $\tau_l(r)$, which in turn allows us to use equation (42) to compute each person's cumulative fallout dose.

Table 1-10 of [1] states that the fallout transmission factor in a vehicle is 0.5-0.7, while pg 6 of [36] claims that vehicles provide virtually no protection from fallout. Vehicles have an air exchange of 7/hr, and so it will not prevent inhalation of fallout either. We assume a radiation transmission factor of $s_v = 0.9$ for people who are in a vehicle.

To compute the number of incremental deaths due to radiation fallout, we apply the dose-response function $P_f(D)$ in equation (28) (or the function $\tilde{P}_f(D)$ defined in §1.4 for people with burn or blast injuries) to the total transmitted prompt plus fallout dose for all survivors, whether they shelter, evacuate by foot or evacuate by vehicle; the people who shelter have random transmission factors as described in (27), people who evacuate by foot receive the full fallout dose, and people who evacuate by vehicle have the transmission factor $s_v = 0.9$. The incremental number of injuries due to radiation fallout is calculated in a similar manner, but the dose-response function $P_i(D)$ in (29) is used, regardless of whether there are burn or blast injuries.

In addition, the maximum survivable exposure increases the lifetime probability of (fatal and non-fatal) cancer from 0.2 to 0.3. Following pg 1-28 of [1], we include a multiplicative factor for survivors of 5×10^{-4} /person-rem for excess latent cancer deaths. These latent deaths are due to prompt and fallout radiation.

4 Delayed Evacuation

For the people who initially shelter in place, we need a strategy for deciding when and how these people should be evacuated. We consider the delayed evacuation of people with vehicles in §4.1 and the delayed evacuation of pedestrians in §4.2.

4.1 Delayed Evacuation of People with Vehicles

For people with vehicles, we need to tell them when and where to evacuate (we may again have some false negatives, but probably much fewer). These vehicles evacuate according to the PDE in §3.3 (i.e., equation (49)). An organized evacuation presumes reliable communication between the government and the evacuators. We assume that there is situational awareness of the plume, and hence consider the avoidance evacuation scheme described at the end of §3.3, where all vehicles are moving away from the fallout zone.

We construct two extreme policies: a high-dose-first policy, which gives evacuation priority to people in areas with high fallout doses, and a low-dose-first policy, which gives evacuation priority to vehicles in areas with low fallout doses. In contrast to the model in §3.3, here we can manage the level of congestion. Consequently, for each of these strategies, we load as many vehicles as possible on the roads, subject to constraints on the amount of congestion.

We view evacuation as a two-stage problem along arcs and then along rays. We use backward induction (as is optimal in sequential decision problems) and hence start with evacuation on the rays (which is described in terms of the ray at angle ϕ). If we use the existing PDE in equation (49), we need to choose the β_i^{ray} values (β_o^{ray} is still defined by (58)). Note that by equation (42), the arcs will be in the priority order $0, 1, \dots$, for the high-dose-first policy (for practical values of t) and will be in the reverse order for the low-dose-first policy. We choose the $\beta_i^{\text{ray}}(r_j, t)$ values using the following iterative greedy algorithm for the

high-dose-first algorithm:

Step 1: Fix the beginning of the evacuation time, τ_e , and set $j = 0$. Let $\rho_{\text{ray}}(r, t)$ be the total vehicle density due to vehicles arriving to the ray from arcs 0. Load all of arc 0 traffic (i.e., all vehicles that enter the ray from arc 0 at some time during the delayed evacuation procedure) onto the ray as fast as possible beginning at τ_e (via the choice of $\beta_i^{\text{ray}}(r_0, t)$), subject to the constraints $\rho_{\text{ray}}(r, t) \leq 166.5$ vehicles/km $\forall r, t$ and $\beta_i^{\text{ray}}(r_0, t)\Delta t \leq \min\{\frac{1}{2}(148.4), \frac{1}{4}(333 - \rho_{\text{ray}}(r_0, t))\}$. These constraints disallow the ray density from exceeding the level at which the maximum flow is achieved, and prevent queueing of vehicles at the arc-ray intersection.

Step 2: Increase j by 1, and redefine $\rho_{\text{ray}}(r, t)$ to be the total vehicle density due to vehicles arriving to the ray from arcs $0, \dots, j$. If $r_j > r_e + 90$ km, then stop. Load arc j traffic onto the ray as fast as possible beginning at τ_e (via $\beta_i^{\text{ray}}(r_j, t)$), subject to the constraints $\rho_{\text{ray}}(r, t) \leq 166.5$ vehicles/km $\forall r, t$ and $\beta_i^{\text{ray}}(r_j, t)\Delta t \leq \min\{\frac{1}{2}(148.4), \frac{1}{4}(333 - \rho_{\text{ray}}(r_j, t))\}$. Go back to the beginning of step 2.

The low-dose-first algorithm is identical to the high-dose first algorithm described above, except that we start at $r_j = r_e + 90$ km, decrease j by 1 at the beginning of step 2, and terminate the algorithm after $j = 0$.

Given the final solution $\rho(r, t)$ to the ray-loading problem, we turn to the arc-loading problem. This is a very similar problem to the ray-loading problem, in that all traffic is moving to lower-dose areas. We use the arc version of PDE (49) with β_o^{arc} values set equal to the β_i^{ray} values derived in the greedy algorithm for the ray-loading problem. We again use a two-step greedy algorithm (for simplicity, we allow arc arrivals to occur every km) subject to the constraints $\rho_{\text{arc}}(r, t) \leq 74.2$ vehicles/km $\forall r, t$, $\beta_i^{\text{arc}}(s, t)\Delta t \leq \frac{1}{2}(148.4 - \rho_{\text{arc}}(s, t))$ (this constraint prevents queue buildups of vehicles waiting to enter an arc), and the additional constraint $\rho_{\text{arc}}(\phi + \frac{\pi}{4}, t) \geq \beta_o^{\text{arc}}(\phi + \frac{\pi}{4}, t)\Delta t$ dictated by (59).

Finally, because solving these loading problems with the PDE in (49) is computationally prohibitive (the constraints need to be checked for all locations and all future times), we approximate the PDE by a system of linear ordinary differential equations (ODEs) in the above algorithm. Consider a ray with arcs $j = 0, 1, \dots$. Let $Q_j(t)$ be the number of vehicles on the ray between arcs j and $j + 1$, let $\lambda_j(t)$ be the loading rate onto the ray from arc j at time t (this is the decision variable), and let μ be the rate at which vehicles proceed from one ray segment to the next (i.e., from the segment between arcs j and $j + 1$ to the segment between arcs $j + 1$ and $j + 2$); we set $\mu = \frac{80\text{km/hr}}{3\text{km}} = 27/\text{hr}$. The system of ODEs is given by

$$\dot{Q}_j(t) = \lambda_j(t) + \mu Q_{j-1}(t) - \mu Q_j(t). \quad (60)$$

We incorporate the exiting off rays in (58) via $\dot{Q}_j(t) = \lambda_j(t) + \frac{29}{30}\mu Q_{j-1}(t) - \mu Q_j(t)$ for $r_j \in [r_e, r_e + 90]$ km. In the algorithm, we replace the ρ_{ray} constraint by $Q_j(t) \leq 500$ vehicles (which equals 166.5 vehicles times 3 km, which is the length of each ray segment) and replace the β_i^{ray} constraint by $\lambda_j(t) \leq \min\{\frac{3}{2}(148.4), \frac{1}{4}(999 - Q_j(t))\}$, again by multiplying densities by 3 km. The constraints in the greedy algorithm for the arcs are $Q_j(t) \leq 3(74.2) = 222.6$ and $\lambda_j(t) \leq \frac{1}{2}(3(148.4) - Q_j(t))$, where j now indexes the arc segments.

4.2 Delayed Evacuation of Pedestrians

In this subsection, we describe how to model public evacuation for people without vehicles who initially sheltered in place. We assume that there are a set of evacuation stations that pedestrians walk to, get decontaminated (although we do not model the decontamination process) and receive transportation to a safe place. In contrast to the evacuation of people with vehicles, the organized evacuation of pedestrians requires substantial human resources in the evacuation area to manage the evacuation stations, perform the decontamination, and drive the transport vehicles (hereafter called buses).

We assume that the locations of the evacuation stations are dictated by the tolerable

total doses for emergency workers, which are 5 rem (0.4% increase in excess cancer rate) for emergency workers doing nonvital activities, 10 rem (0.8% excess risk) for non-lifesaving activities such as protecting major critical infrastructure, and 50 rem (4% excess risk) for lifesaving activities [37]. We set the fallout dose rate threshold to 10 rem/hr, so that each worker could spend 5 hr at the site (including transportation to and from the evacuation station).

Our pedestrian evacuation model has one free variable, which is the evacuation time τ_e . We compute the dose contour $\{(x, y) | D_e(x, y, \tau_e) = 10 \text{ rem/hr}\}$. Because evacuation shelters need to be located beyond the blast and burn zones, we compute the intersection of the region inside the contour and the region $r > 1.5 \text{ km}$, and then assume that evacuation stations are placed at the perimeter of the intersection of these two regions; we refer to the intersection of these two regions as the evacuation region. We assume that any pedestrian evacuee who is located outside of the evacuation region is immediately evacuated without incurring any additional fallout dose.

We assume that delayed pedestrian evacuees who are inside of the evacuation region begin walking at 1 mph at time τ_e . If ψ is the direction of the shortest path from a person's location to the perimeter of the evacuation region, we assume that each person moves in a random direction that is uniformly distributed in $[\psi - \frac{\pi}{16}, \psi + \frac{\pi}{16}]$. When an evacuee's path intersects the perimeter of the evacuation region, we assume that he is immediately at an evacuation station; hence, the random angle is intended to crudely account both for evacuees not taking the shortest path to their destination, and the fact that these evacuation stations are set up only at discrete locations along the perimeter of the evacuation region.

The time from a person's arrival to an evacuation station until he is safely transported outside of the fallout zone depends upon the exact number of evacuation stations, the number of workers at these stations, the number of buses used to transport people out of these

stations, and the congestion that these buses experience on the roads. We ignore all of these details and compute only the total fallout dose incurred by a person until he gets to an evacuation station. Hence, our casualty estimates for delayed pedestrian evacuation are lower bounds, and essentially assume that people are either well sheltered (from fallout) as soon as they arrive to an evacuation station or that there are ample buses (so there is no waiting time at the evacuation station), and that buses incur very little traffic congestion (e.g., some of the inbound lanes on the rays are devoted to these buses and other emergency vehicles).

References

- [1] Department of Homeland Security. National planning scenarios. Washington, D.C., April 2005. Accessed at <http://media.washingtonpost.com/wp-srv/nation/nationalsecurity/earlywarning/NationalPlanningScenariosApril2005.pdf>.
- [2] Glasstone, S., P. J. Dolan. The effects of nuclear weapons, third ed. U.S. Department of Defense and Energy Research and Development Administration, Washington, D.C., 1977.
- [3] Davis, L. W., F. J. Wall, D. L. Summers. Development of “typical” urban areas and associated casualty curve. Report DC-FR-1041, Dikewood Corp., Albuquerque, NM, 1965.
- [4] Lewis, J. A Review of DHS NAL planning scenario for a 10-kiloton nuclear detonation on Washington, DC. March 2006.
- [5] Defense Nuclear Agency. Effects manual number 1: capabilities of nuclear weapons. Ed., P. J. Dolan. Washington, D.C., 1972.
- [6] Brode, H. L., R. D. Small. A review of the physics of large urban fires. In *The medical implications of nuclear war*, Institute of Medicine, National Academy Press, Washington, D.C., 1986.
- [7] Office of the Surgeon General, Department of the Army. Medical consequences of nuclear warfare: textbook of military medicine, part I, volume 2. Eds., R. I. Walker, T. J. Cerveney. 1989.
- [8] Daugherty, W., B. Levi, F. Von Hippel. Casualties due to the blast, heat, and radioactive fallout from various hypothetical nuclear attacks on the United States. In *Medical*

implications of nuclear war, Institute of Medicine, 207-232, National Academy Press, Washington, D.C., 1986.

- [9] Institute of Medicine. Assessing medical preparedness to respond to a terrorist nuclear event: workshop report. Benjamin, G. C., M. McGeary, S. E. McCutchen, eds. National Academies Press, Washington, D.C., 2009.
- [10] Buddemeier, B. Improving response to the aftermath of radiological and nuclear terrorism. Lawrence Livermore National Laboratory LLNL-PRES-404937-rev1, Livermore, CA, June 2008.
- [11] LandScan USA. Accessed at www.ornl.gov/sci/landscan/ on October 1, 2009.
- [12] Marrs, R. E. Radioactive fallout from terrorist nuclear detonations. Lawrence Livermore National Laboratory report UCRL-TR-230908, Livermore, CA, May 11, 2007.
- [13] Nasstrom, J. S., G. Sugiyama, R. L. Baskett, S. C. Larson, M. M. Bradley. The National Atmospheric Release Advisory Center (NARAC) modeling and decision support system for radiological and nuclear emergency preparedness and response. Lawrence Livermore National Laboratory report UCRL-JRNL-211678, Livermore, CA, April 2005.
- [14] Marrs, R. E. Personal communication, June 29, 2009.
- [15] Bresee, J. C., D. L. Narver, Jr. Improved shelters and accessories. Chapter 9 in *Survival and the Bomb: methods of civil defense*, Ed. E. P. Wigner, Indiana University Press, Bloomington, IN, 1969.
- [16] Meade, C., R. C. Molander. Considering the effects of a catastrophic terrorist attack. Rand Corporation TR-391-CTRMP, Santa Monica, CA, 2006.

- [17] Carter, A. B., M. M. May, W. J. Perry. The day after. A report based on a workshop hosted by The Preventive Defense Project, Stanford University, Stanford, CA, 2007.
- [18] Vogt, B. M., J. H. Sorenson. Description of survey data regarding the chemical repackaging plant accident West Helena, Arkansas. ORNL/TM-13722, Oak Ridge National Laboratory, Oak Ridge, TN, March 1999.
- [19] Sorenson, J. H., B. M. Vogt. Emergency evacuation handbook. Oak Ridge National Laboratory, Oak Ridge, TN, February 2006.
- [20] Lindell, M. K., C. S. Prater. Critical behavioral assumptions in evacuation time estimate analysis for private vehicles: examples from hurricane research and planning. *J. Urban Planning Development* **133**, 18-29, 2007.
- [21] Stern, E., A. Sinuany-Stern. A behavioral-based simulation model for urban evacuation. *Papers Regional Science Association* **66**, 87-103, 1989.
- [22] U.S. Census Bureau. American community survey 2006, Table S0802.
- [23] District Department of Transportation. District response plan: emergency transportation annex. Washington, DC, August 2006.
- [24] Dombroski, M. J., P. S. Fischbeck. An integrated physical dispersion model and behavioral response model for risk assessment of radiological dispersion device (RDD) events. *Risk Analysis* **26**, 501-514, 2006.
- [25] Larson, R. C., A. R. Odoni. *Urban operations research*. Prentice-Hall, Inc., Englewood Cliffs, NJ, 1981.
- [26] Road map of Washington DC, Beltway. Accessed at www.aaccessmaps.com/show/map/us/dc/dcmetro_beltway on November 4, 2009.

- [27] Sheridan, M. B. Guide to evacuate region reveals limitations. *Washington Post*, pg B01, February 4, 2008.
- [28] Federal Highway Administration. The 1985 highway capacity manual. U.S. Department of Transportation, Washington, DC, April 1986.
- [29] U.S. Census Bureau. County-to-county worker flow files. *Census 2000*.
- [30] Murray,-Tuite, P. M., H. S. Mahmassani. Transportation network evacuation planning with household activity interactions. *Transportation Research Record*, no. 1894, 150-159, 2004.
- [31] Lighthill, M. J., G. B. Whitham. On kinematic waves II. A theory of traffic flow on long crowded roads. *Proceedings Royal Society London*, **A229**, 317-345, 1955.
- [32] Haberman, R. Mathematical models: mechanical vibrations, population dynamics, and traffic flow. Prentice-Hall Inc., Englewood Cliffs, NJ, 1977.
- [33] Sheffi, Y., H. Mahmassani, W. B. Powell. A transportation network evacuation model. *Transportation Research* **16A**, 209-218, 1982.
- [34] Harrison, J. M. *Brownian motion and stochastic flow systems*. John Wiley & Sons, New York, 1985.
- [35] Daganzo, C. F. The cell transmission model: a dynamic representation of highway traffic consistent with the hydrodynamic theory. *Transportation Research B* **28B**, 269-287, 1994.
- [36] Bell, W. C., C. E. Dallas. Vulnerability of populations and the urban health care systems to nuclear weapon attack - examples from four American cities. *Int. J. Health Geographics* **6**, 5, 2007.

- [37] Conference of Radiation Control Program Directors, Inc. Handbook for responding to a radiological dispersal device: first responder's guide - the first 12 hours. CRCPD Publication 06-6, September 2006.

Subscript	Range of r	μ	$F(0)$
N	(0,2500)	0.0047	e^{22}
N	[2500,5000)	0.0047	e^{22}
γs	(0,2500)	0.0034	e^{20}
γs	[2500,5000)	0.0034	e^{20}
γf	[500,1500)	0.0057	$e^{9.2}$
γf	[1500,2500)	0.0046	$e^{7.8}$
γf	[2500,5000)	0.0042	$e^{6.8}$

Table 1: Values of μ and $F(0)$ for the three categories of radiation, as a function of the distance r from the blast.

x distance (km)	$A(x)$	$\delta(x)$	$\Delta(x)$	$c(x)$
5	0.93	0.48	3.8	2.3
10	0.88	0.71	3.8	2.5
15	0.88	0.92	3.8	3.0

Table 2: Values of the plume width parameters in equation (42) as a function of the distance along the wind direction (x) from the detonation. Data obtained from [14].

Figure Legends

Fig. 1: Spatial probability of fatalities (—) or injuries (- - -) due to **(a)** blast effects, **(b)** thermal effects, **(c)** prompt radiation, and **(d)** combined effects.

Fig. 2: The fallout death and injury rate vs. the time at which delayed evacuation of pedestrians is initiated (τ_e), when personal situational awareness is **(a)** low ($r_p = 4$ km) and **(b)** high ($r_p = 17$ km).

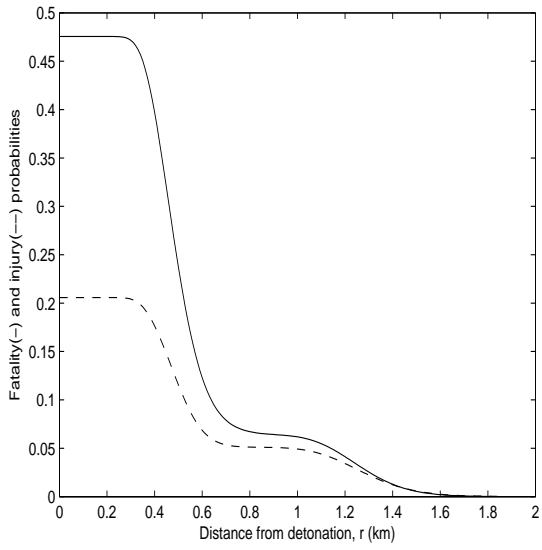
Fig. 3: Spatial comparison of self-evacuation vs. delayed evacuation when $\tau_e = 12$ hr and $r_p = 4$ km. Each location (x, y) is categorized in one of three ways: the death probability is the same for self-evacuation and delayed evacuation ($\Delta(x, y) = 0$), the death probability is higher for self-evacuation ($\Delta(x, y) > 0$), or the death probability is higher for delayed evacuation ($\Delta(x, y) < 0$). The dose contours dictating the location of the evacuation stations for four values of τ_e are displayed, with the exception that evacuation stations cannot be within 1.5 km of the blast.

Fig. 4: Under the assumption that delayed evacuation offers neither improved situational awareness (via a narrower range of walking angles) nor less fallout exposure (via evacuation stations), we compute the optimal value of $\tau_e(x, y)$, which is the time to initiate delayed pedestrian evacuation from location (x, y) .

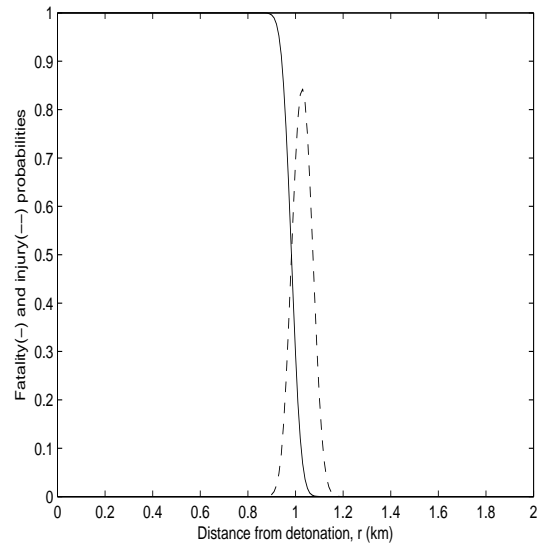
Fig. 5: Delayed vehicle evacuation when everyone initially shelters. The number of deaths vs. the time that delayed vehicle evacuation is initiated (τ_e) under the assumption that $n(\bar{D}_e) = f_n = f_p = 0$; i.e., all prompt survivors with access to a vehicle initially shelter in place.

Fig. 6: Delayed vehicle evacuation for varying false positive probabilities. With the false negative probability $f_n = 0.05$ and the delayed evacuation time $\tau_e = 24$ hr, for each value of the false positive probability f_p we choose the death-minimizing value of \bar{D}_e and plot the

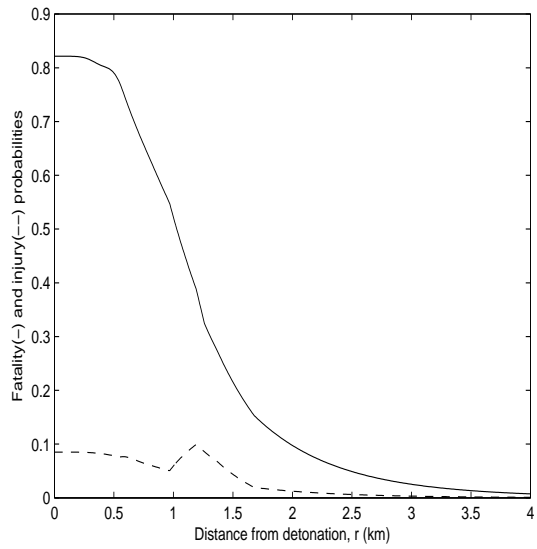
number of deaths vs f_p . The optimal value of $n(\bar{D}_e^*)$ is 39.1k for $f_p \leq 0.95$.



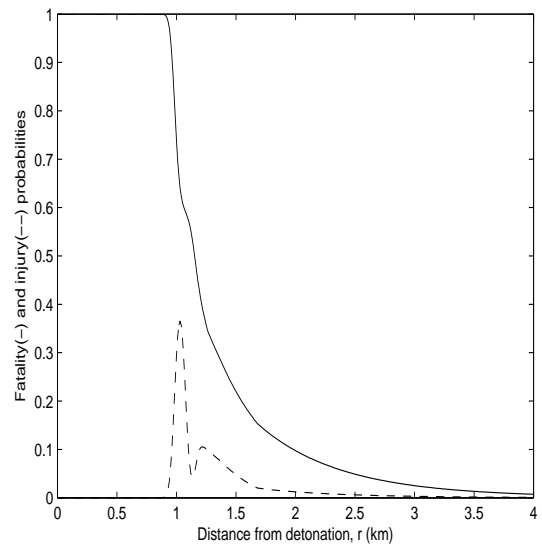
(a)



(c)

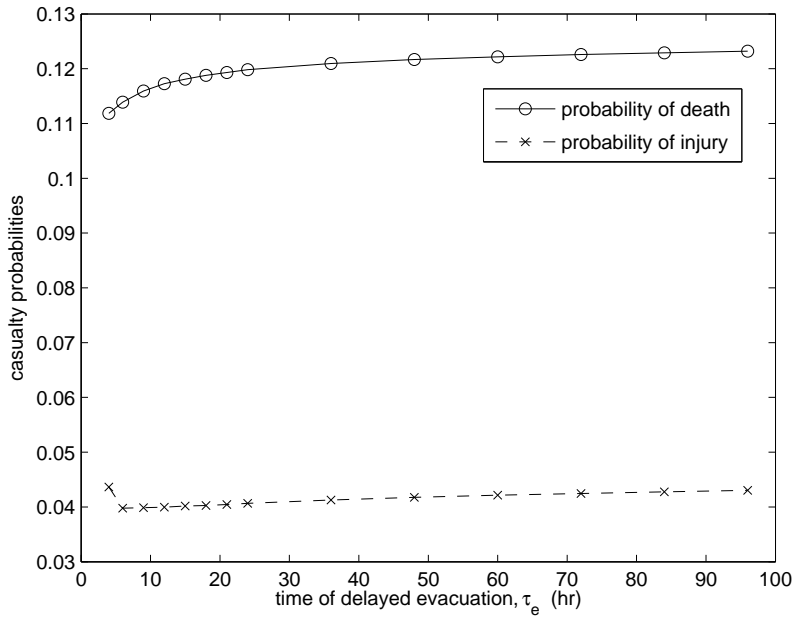


(b)

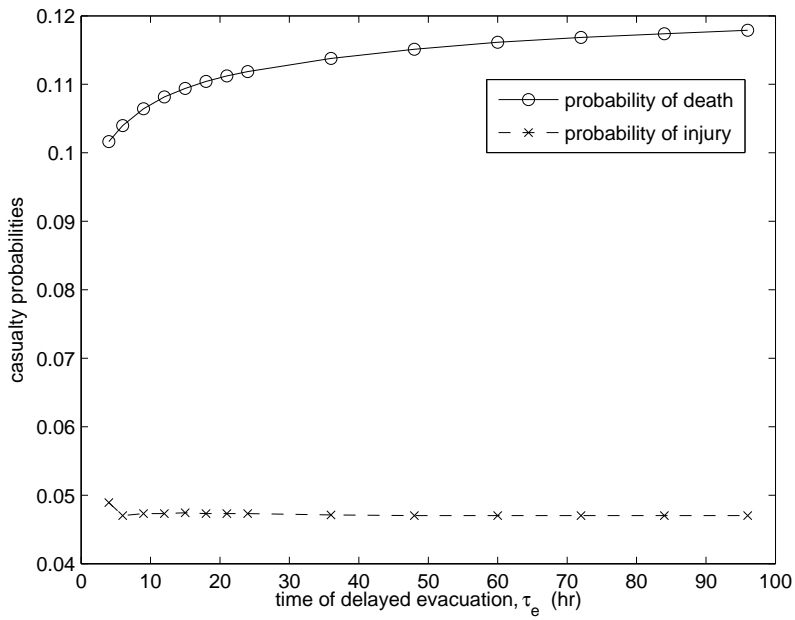


(d)

Figure 1:



(a)



(b)

Figure 2:

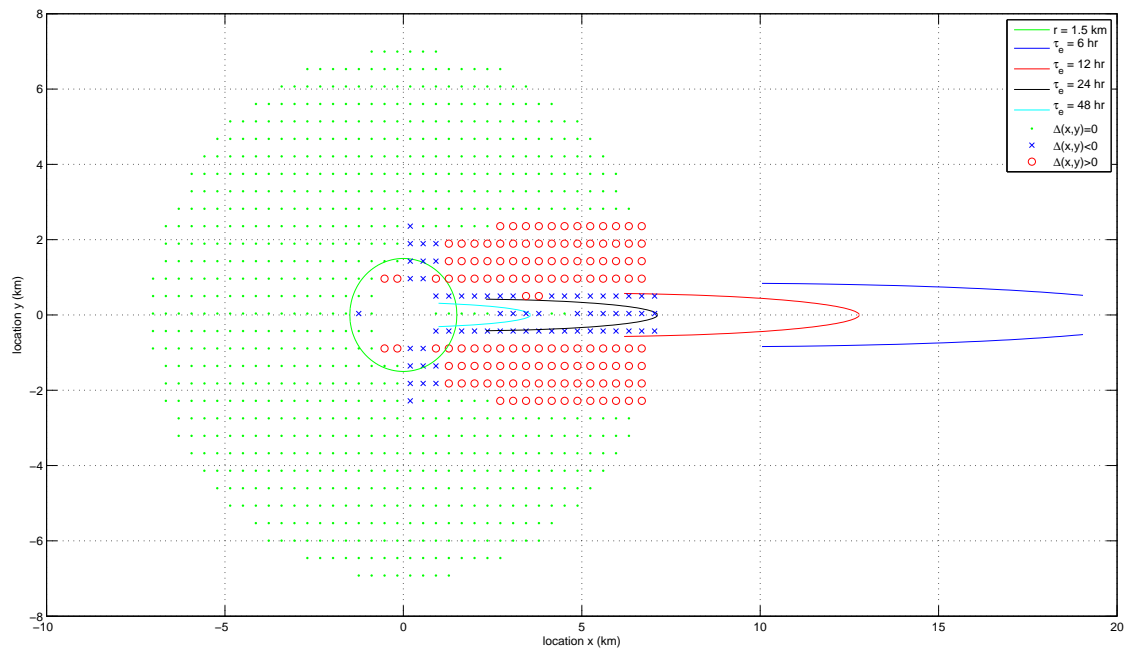


Figure 3:

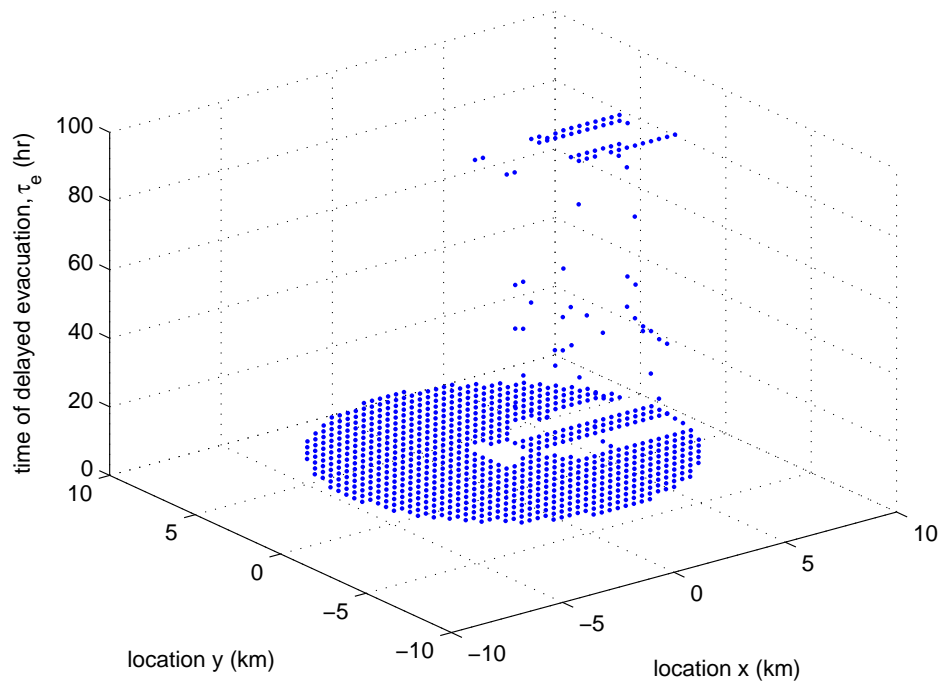


Figure 4:

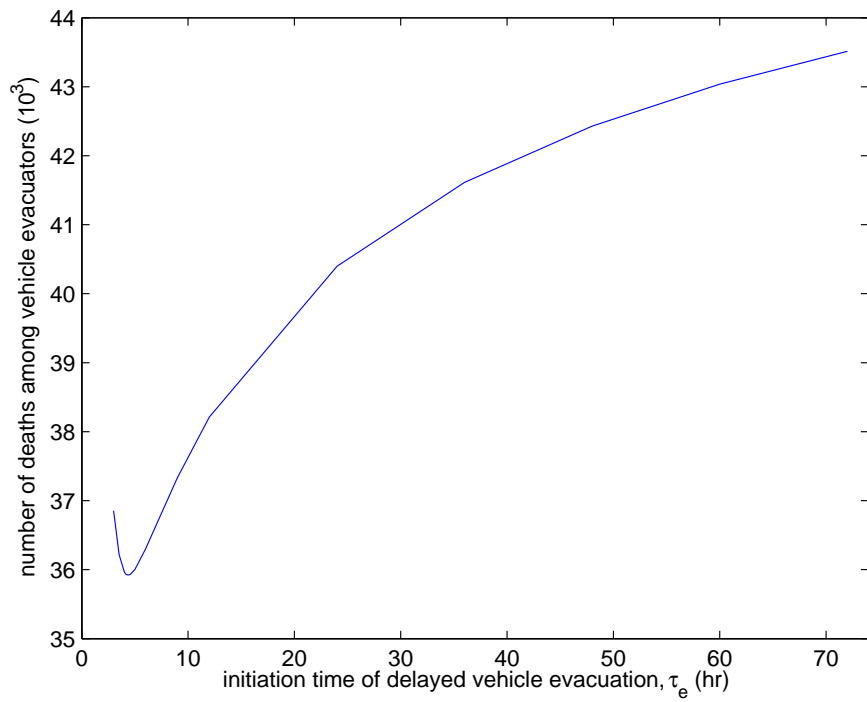


Figure 5:

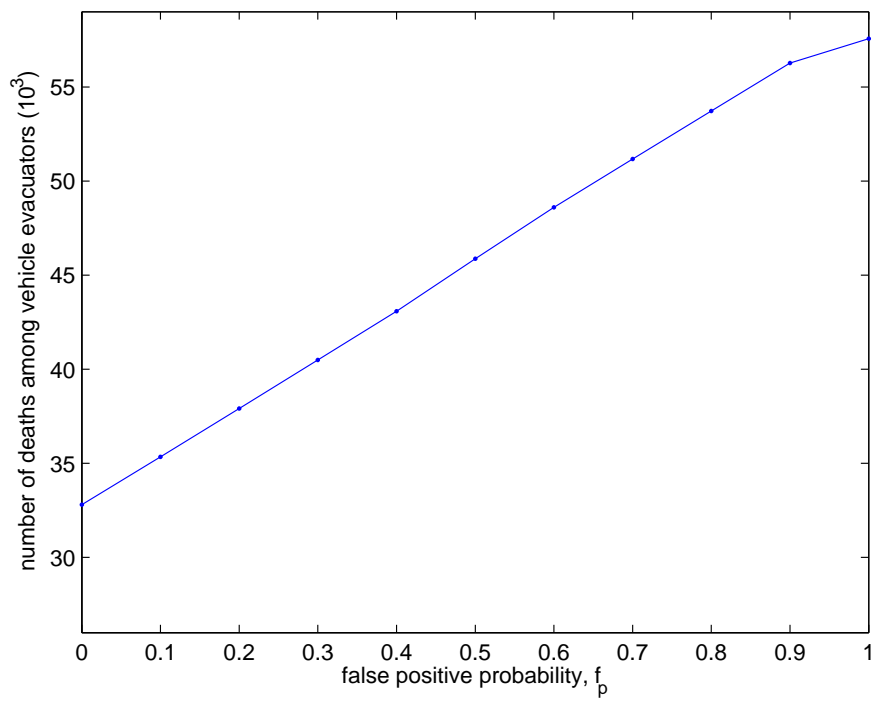


Figure 6: